Multijet Electrospinning of Conducting Nanofibers from Microfluidic Manifolds

Yasmin Srivastava,[1,2] Manuel Marquez,[2–4] Todd Thorsen[1]

[1]*Department of Mechanical Engineering, Massachusetts Institute of Technology, Cambridge, Massachusetts 02139-4307*
[2]*INEST Group, Research Center, Philip Morris USA, Richmond, Virginia 23234*
[3]*NCTCN Center, Physical and Chemical Properties Division, NIST, Gaithersburg, Maryland 20899*
[4]*Harrington Department of Bioengineering, Arizona State University, Tempe, Arizona 85287*

Received 5 January 2007; accepted 12 May 2007
DOI 10.1002/app.26810
Published online 14 August 2007 in Wiley InterScience (www.interscience.wiley.com).

ABSTRACT: We present a method for the electrospinning of conducting polymeric composite nanofibers using a poly(dimethyl siloxane) (PDMS)-based microfluidic device. To scale-up the process and spin multicomponent systems, we designed a unique multi-spinnerette electrospinning device using microchannels cast in PDMS. Nanofibers of poly (vinylpyrrolidone) and its composite with polypyrrole were successfully prepared using one-step and two-step microfluidic electrospinning. The effect of processing variables on the morphology of the nanofibers formed using this device was also studied. SEM images showed that fiber diameter and morphology strongly depend on processing parameters such as concentration, applied electric field, feed rate, solvent, and ionic salt addition. FTIR spectroscopy and conductivity measurements reveal the polymerization of pyrrole in the matrix of poly(vinyl pyrrolidone). © 2007 Wiley Periodicals, Inc. J Appl Polym Sci 106: 3171–3178, 2007

Key words: microfluidic; composites; conducting polymers; morphology; multijet

INTRODUCTION

Advances in the fields of electronics, optics, and medicine have motivated the production of a variety of nanodimensional functional materials ranging from thin films to fibers. The versatile technology of electrospinning for the preparation of polymer nanofibers has been known since early 1930s.[1] In the conventional electrospinning method, a syringe with a fixed diameter of 0.3–1 mm has been used as an electrospinning source.[2] The pendant polymeric droplet exiting the tip of the needle, when subjected to strong electric field, will deform into a Taylor cone and form a liquid jet. The jet undergoes an electrically-induced bending instability which results in strong looping and the stretching of the jet. After the solvent evaporation, ultrathin fibers are deposited on the counter electrode. Since then, a number of techniques combined with electrospinning have been reported, including co-electrospinning of different polymer solutions by coaxial two-capillary spinnerets,[3–5] scanning tip source,[6] coating template nanofibers using CVD,[7] upward needleless electrospinning,[8] polymer/ceramic uniaxially aligned arrays,[9,10] and the mixture of polymer solutions with nanomaterials.[11–13] However, reports on multijet electrospinning are limited,[14–17] and are mainly restricted to side-by-side electrospinning with multiple syringes, porous tubes or pipes. In this communication, we describe the development of a multichannel microfluidic device in poly(dimethyl siloxane) (PDMS) for the parallel electrospinning of single and conducting composite nanofibers. Advantages of this technology over conventional syringe-based methods include rapid prototyping, ease of fabrication and parallel electrospinning with in a single, monolithic device. Fabricating a complex network of microchannels for multicomponent electrospinning is easily accomplished using PDMS–based micromolding technology. User friendly designs like the tree design in the current study also provides the flexibility of having multiple outputs with one single input.

Polyvinylpyrrolidone (PVP) is an important synthetic polymer with excellent physiological compatibility and reasonable solubility in water and other organic solvents, with applications in pharmaceuticals, cosmetics, detergents, paints, and biological engineering. Furthermore, among the range of conducting polymers, polypyrrole (PPy) has been widely used for sensors and biosensing applications.[18–20] While several reports on electrospinning of PVP nanofibers using conventional syringe method have been reported,[21,22] the electrospinning of PPy is limited by its insolubility and intractability.[23] Although

Correspondence to: T. Thorsen (thorsen@mit.edu).
Contract grant sponsor: Philip Morris USA (INEST grant).

PPy has high electrical conductivity and good environmental stability, it lacks processibility.[24] Hence, the advantages of polypyrrole could be exploited by blending it with an appropriate polymer like PVP, which has good solubility. Polymerization of pyrrole monomer into a host polymer matrix[25] and blending of other conjugated polymers with host polymers to improve their processibility and performance has been reported by several researchers.[26–28]

In this article, we report on the electrospinning of PVP and PVP/PPy composite nanofibers using microfluidic manifolds. To gain a better understanding of the correlation between synthesis conditions and fiber morphology for single component (PVP) nanofibers, nanofibers were generated using microfluidic manifolds, altering parameters such as polymer concentration, solvent type, feed rate, voltage, and the presence of salt. Optimization of the processing conditions for PVP nanofibers was subsequently applied to the synthesis of composite PVP/PPy nanofibers. Two methods to fabricate PVP/PPy composite nanofibers were utilized. In the first method, PVP, pyrrole, and ferric chloride ($FeCl_3$) were spun together as a composite mixture, with pyrrole polymerization driven by $FeCl_3$ in the matrix of PVP. $FeCl_3$ is an efficient oxidant for pyrrole polymerization, doping chlorine ions in the PPy to make it electrically conducting. In the second method, PVP nanofibers containing $FeCl_3$ were spun together followed by vapor phase polymerization of pyrrole in the PVP matrix.[29,30]

EXPERIMENTAL

Materials

PVP (average MW 1300 kD) was procured from ACROS Organics, pyrrole monomer (98 +%) from Alfa Aesar, ferric chloride, 6-Hydrate (98.3%) from J.T Baker, *N*,*N*-dimethylformamide (99.9 +%) from Honeywell International (B & J Brand), and ethyl alcohol (99.98%) from pharmco-AAPER were used.

Microfluidic device fabrication

Microfluidic devices for electrospinning were molded in PDMS using established soft lithography methods.[31] To make the mold, a 100 μm thick layer of SU8 photoresist (Microchem) was spun on the silicon wafer. The SU8 layer was given a pre-exposure bake of 10 min at 65°C and 30 min at 95°C. It was subsequently exposed to UV-irradiation through the transparency mask and baked for 1 min at 65°C and 10 min at 95°C prior to development. To prevent the PDMS from sticking to the mold, a silanizing agent (chloro-trimethyl-silane) was deposited on the mold. Once the mold was made and silanized, PDMS (Dow Corning Sylgard 184 Silicone) base was mixed thoroughly with the included curing agent in the ratio of 5 : 1 respectively and poured over the mold placed in a Petri dish. It was then degassed and cured at 80°C for 1 h. After curing, the devices were peeled from the molds and the interconnects were created by coring holes using a 20-gauge flat tip needle (McMaster Carr). Once the holes for interconnects were created, the devices were sealed with a partially-cured thin layer or PDMS and cured overnight at 80°C. The channels dimensions of the device were $\sim$ 100 μm (w) $\times$ 100 μm (h).

Electrospinning device configuration

Figure 1(A) illustrates the schematic setup for the electrospinning of nanofibers of PVP and its composite with PPy. The configuration is same as conventional electrospinning except that the syringe is replaced with a microfluidic device [Fig. 1(B,C)]. In this setup, the polymer solution is continuously fed through the microfluidic device using a syringe pump (Model 11plus of Harvard Apparatus). A high voltage of 10–15 kV is applied using a high voltage supply, ES 30P-10W of Gamma High Voltage Research Inc. The distance between the source and the collector was 10 cm.

One-step electrospinning of PVP and PVP/PPy composite nanofibers

A PVP (MW 1,300,000) solution was prepared by dissolving PVP in ethanol, dimethylformamide (DMF), and mixed solvent of (1 : 1 v/v) ethanol : DMF at various concentrations of PVP (1–8% w/v) and magnetically stirred for 24 h at room temperature prior to electrospinning. The polymer solution was fed through the device at the rate of 0.01 mL/min. Using applied voltages ranging from 10–20 kV, nanofibers of PVP were collected on silicon wafers placed on the collector. For PVP/PPy composite nanofiber synthesis, 1*M* pyrrole was added to a mixture of PVP (4% w/v) and $FeCl_3$ (10% w/v) in (1 : 1 v/v) ethanol : DMF. In the presence of $FeCl_3$, pyrrole polymerizes in the matrix of PVP forming a conducting composite. $FeCl_3$ and pyrrole monomer concentrations were optimized to get conducting nanofibers.

Two-step electrospinning of PVP/PPy nanofibers

PVP/$FeCl_3$ solutions were prepared at room temperature by dissolving a mixture of PVP (4%) and $FeCl_3$ (10%) by weight in (1 : 1 v/v) ethanol : DMF. The PVP/$FeCl_3$ solution was homogenized by constant stirring for 24 h and then fed through the device for electrospinning. The electrospun nanofibers of PVP/

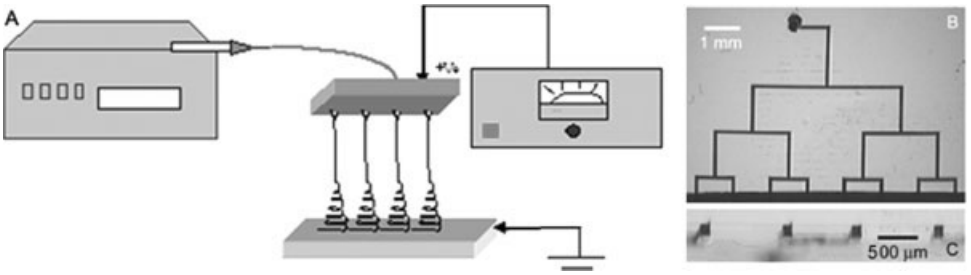

Figure 1 (A) Schematic diagram of microfluidic electrospinning using a branching microchannel architecture to simultaneously spin multiple fibers directly from the channel outlets. (B) Close-up of top side of the poly(dimethy-siloxane) (PDMS) device with channels filled with food coloring to enhance contrast. (C) Side-on cross-section of the device, showing the channel outlets.

$FeCl_3$ were exposed to saturated vapors of pyrrole under ambient conditions. The exposure time was varied from 3 h to 10 days. The oxidative polymerization of pyrrole in the matrix of PVP was confirmed with FTIR spectroscopy. The morphology and dimensions of the fibers were determined using Philips XL30 FEG ESEM and JEOL200CX TEM. FTIR measurements were done using ThermoNicolet Magna 860 FTIR with Spectra-Tec Nic- Plan IR-microscope with ZnSe ATR.

Conductivity measurement

The micro four-point probe conductivity test of the nanofibers was performed by collecting the nanofibers on interdigitated platinum micro-electrodes patterned on glass. A constant current source (Keithley model 2400) was used to pass a steady current through the two outer probes and the voltage drop across the inner two was measured. The conductivity values were calculated from the measured resistance values, distance between the electrodes and the approximate thickness of the nanofibrous mat. The two-point probe measurements were done in a parallel plate configuration of nanofibrous mat sandwiched by two gold electrodes (area $\sim$ 1 cm^2) patterned on glass.[32] A DC power supply (Agilent E3612A) was used to create a voltage, and the current across the sample thickness was measured with a 602 Solid State Electrometer (Keithley Instruments). Before measuring the conductivity, the fiber samples were conditioned for 24 h in (23 $\pm$ 1)°C and 25% relative humidity. Each fibrous mat sample was measured 20 times at different points by applying a potential of 100 V and average values are taken.

RESULTS AND DISCUSSION

The microfluidic device source integrated with the electrospinning technique was successfully able to fabricate nanofibers of PVP and its composite with PPy. The multichannel device has the potential for multijet electrospinning of nanofibers in one small chip at the same time (Fig. 1). In the current microfluidic multi-spinneret arrangement, it was observed that mutually interacting electrified jets still undergo bending instabilities characteristic of electrospinning. In addition, it was found that the jets are repulsed from their neighbors because of coulombic forces. Reasonable stability was achieved by increasing the inter-nozzle distance to $\sim$ 8 mm, yielding more uniform and dense nanofibrous mats. The 8-spinnerette device used in this study produced nanofibers at the rate of 0.1 g/h as against the single needle which produced nanofibers at the rate of 0.02 g/h. The relationship between processing parameters such as concentration, salt, solvent, voltage, feed rate, and morphology of PVP nanofibers fabricated using this microfluidic device are subsequently discussed.

Polymer concentration

In the present study, solutions of PVP in ethanol/DMF produced nanofibers in the concentration range of 2–6% (w/v). Concentrations below 2% generated a mixture of fiber and droplets. Solutions with lower concentrations did not have enough chain entanglement to withstand the electrostatic and coulombic repulsive forces, leading to breaking up of the jet into discrete spheres, while concentrations higher than 6% limit the flow of polymer solution through the channels due to high viscosity. It was observed that, in this processing range of 2–6%, fiber morphology and diameter varied [Fig. 2(A,B)]. There was an increase in average fiber diameter as the concentration increased from 2 to 6% (Table I). This was in accordance with reported literature.[33–36] At lower concentrations (2–3% w/v), the fibers were irregular with average diameter of 200 nm. At higher concentrations (4–6% w/v), fibers were more uniform and cylindrical with fewer junctions, with average diameter of 350 nm. At higher polymer concentrations, lower solvent content dries the fibers completely before they reach the collector, resulting in lower

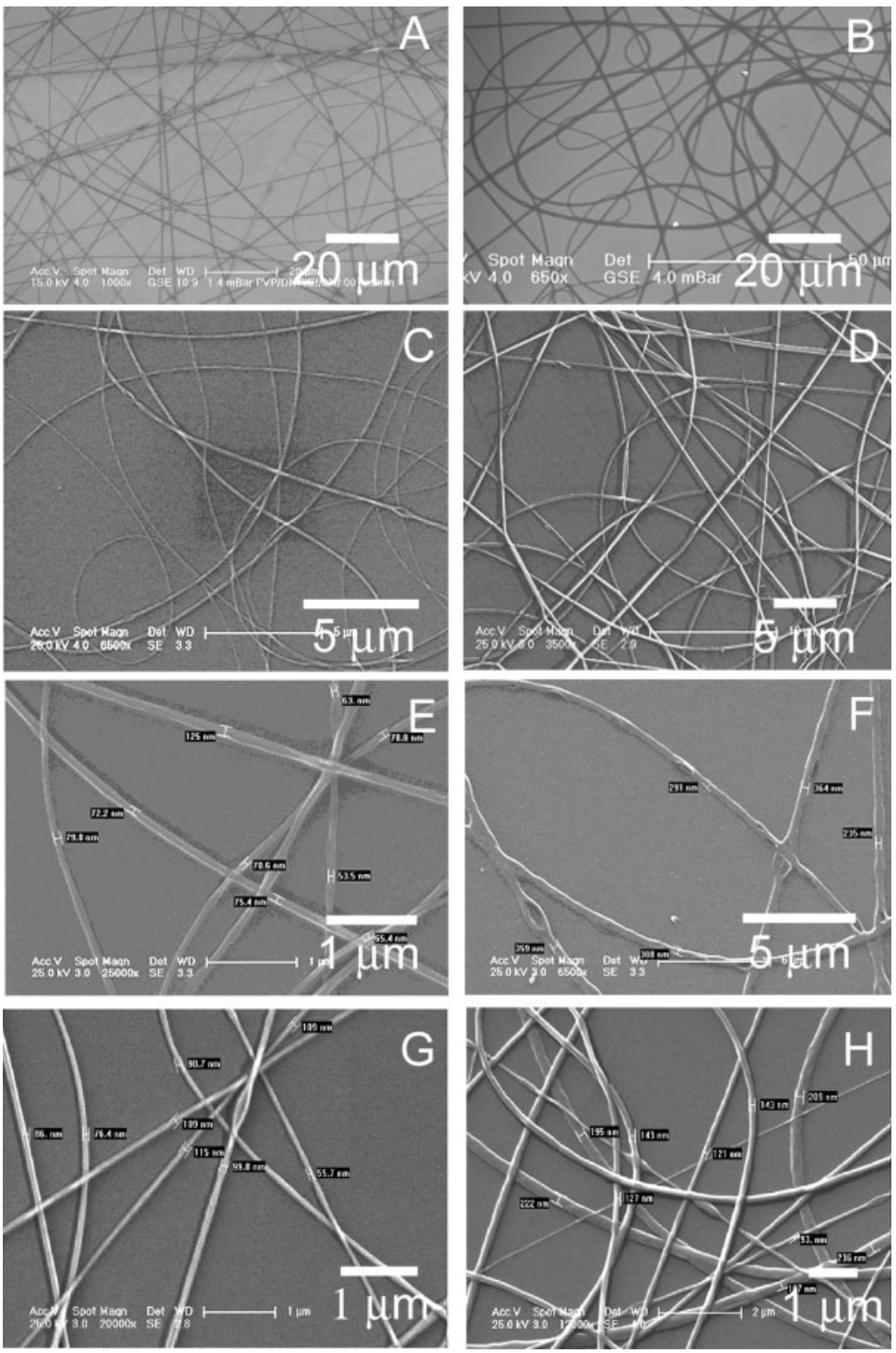

Figure 2 Variation in the morphology and dimension of PVP nanofibers in ethanol/DMF electrospun under different processing conditions; (A) 2% PVP (w/v) (B) 6% PVP (w/v) (C) 4% PVP (w/v) in ethanol/DMF with 10% (w/v) $FeCl_3$ (D) 4% PVP (w/v) (no $FeCl_3$) (E) 4% PVP (w/v) formed at a feed rate of 0.007 mL/min (F) 4% PVP (w/v) formed at a feed rate of 0.1 mL/min (G) 4% PVP (w/v) formed at 10 kV (H) 4% PVP (w/v) formed at 20 kV.

fiber entanglement and a reduction in fiber–fiber junctions. Also, as the polymer concentration increases, viscoelastic forces increase. These viscoelastic forces oppose the electrostatic force that tries to stretch the jet, leading to the formation of thicker fibers.

Salt effects

Nanofibers spun from PVP with 10% $FeCl_3$ exhibited small average diameters ($d_{ave} \sim 100$ nm) as compared to PVP nanofibers without $FeCl_3$ ($d_{ave} \sim 200$

TABLE I
Values of Fiber Diameters of PVP Nanofibers for Different Process Parameters

Process parameters		Average diameter (nm)
Concentration of PVP (w/v)	2%	200
	4%	250
	6 %	350
Voltage (kV)	10 kV	100
	20 kV	250
Flow rate (mL/min)	0.007 mL/min	100
	0.1 mL/min	300
Solvent	Ethanol	300
	DMF	150
	Ethanol + DMF (1 : 1 v/v)	200
$FeCl_3$ (w/v)	0%	200
	10%	100

nm) [Fig. 2(C,D) and Table I]. The solution conductivity affects the electrical force, which may act on a jet causing it to elongate during electrospinning. The addition of salts gives rise to increased charge density of the jet, which in turn results in higher elongation forces on the jet yielding thinner uniform fibers.[33]

Feed rate

In the present investigation, the feeding rate was varied from 0.007 to 0.1 mL/min. For lower feed rates, the fibers were relatively thin and smooth as compared to fibers produced at higher feed rates [Fig. 2(E,F)]. At feed rate of 0.1 mL/min, splaying of droplets and the formation of microholes on the surface of fibers was observed. At higher feed rates, the droplet suspended at the tip is large; as a result, the electrospun nanofibers are still wet when they reach the collector and are thick with have many junctions, similar to the observations of Zong et al.[36]

Electrospinning voltage

It has been observed that variation in applied voltage significantly alters the shape of the initiating droplet, resulting in a change in fiber morphology. In the present studies, the initiating jet was formed when the voltage exceeded 8 kV. For PVP solution of 4% w/v, at a feed rate of 0.01 mL/min, the morphologies of the PVP nanofibers obtained at potentials of 10 and 20 kV are shown in Figure 2(G,H). At lower potential (10 kV), the droplet remains suspended at the exit of the channels and the diameter of the droplet is larger than the channel dimension. At this point, the jet originates from the Taylor cone[37,38] at the bottom of the droplet, and the nanofibers produced have a cylindrical morphology with few bead defects. As the voltage is increased, the polymer solution flow rate exceeds the rate at which steady, uniform electrospinning occurs, making the Taylor cone asymmetrical. Under these conditions, it appears that the jet originates from inside the channel, producing fibers that have an increased density of bead defects.[35,36] Furthermore, SEM images reveal that PVP nanofibers synthesized at higher applied voltages exhibit higher average diameters, which may be due to increase in drawing rate of the jet from the channel. The average diameter of the nanofibers increased from 100 nm (10 kV) to 250 nm (20 kV).

Solvent

SEM images of PVP nanofibers spun from ethanol, DMF, and ethanol/DMF (1 : 1 v/v) show that their morphologies strongly depend on solvent properties such as surface tension, viscosity, charge density, and boiling point of the solvent. It was observed from the SEM images [Fig. 3(A–C)] that PVP nanofibers spun from ethanol were smooth with diameters ranging from 150 to 650 nm ($d_{ave} \sim 300$ nm).

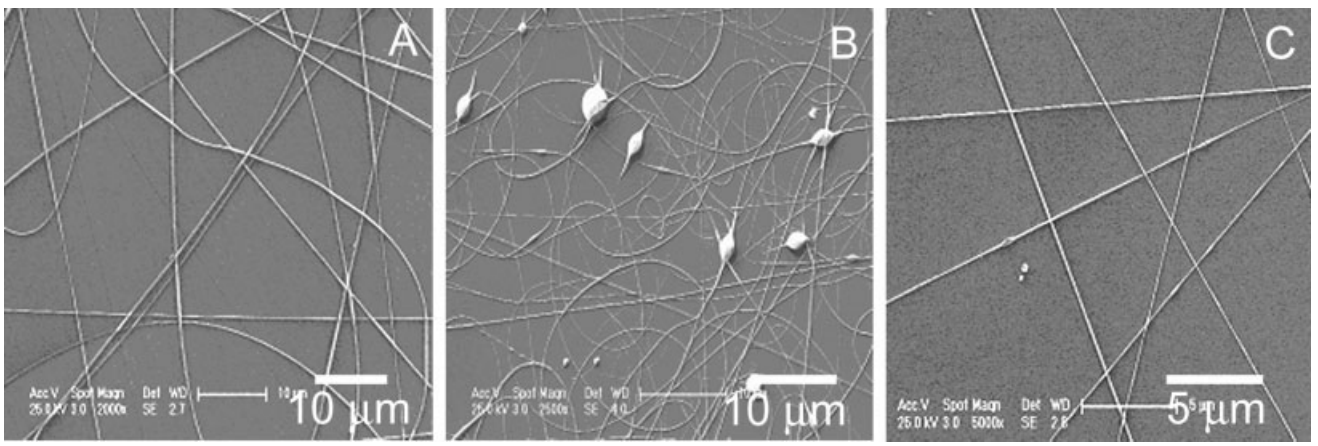

Figure 3 SEM images of 4% PVP (w/v) nanofibers spun in different solvents; (A) ethanol (B) DMF and (C) ethanol/DMF (1 : 1 v/v).

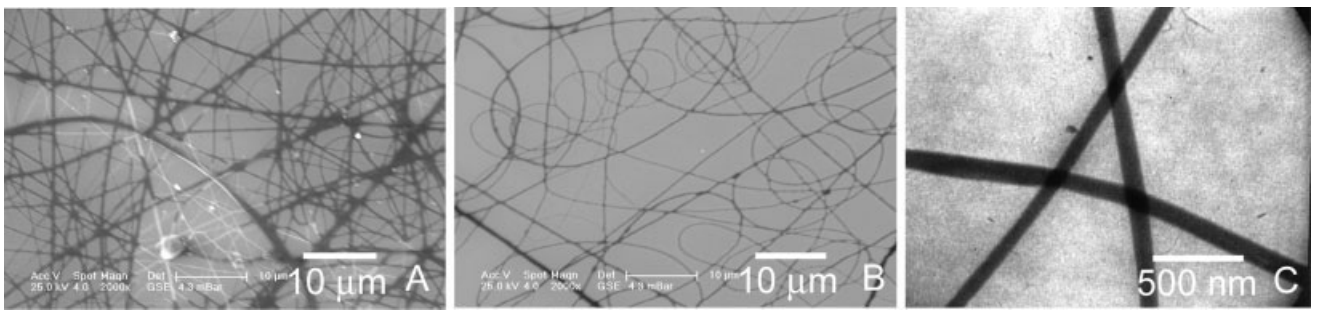

Figure 4 PVP/PPy composite nanofibers: (A) SEM of two-step fabricated PVP/ PPy composite nanofibers (B) SEM of one-step fabricated PVP/PPy composite nanofibers (C) TEM of one-step fabricated PVP/PPy composite nanofibers.

Ethanol makes the solution viscosity higher (54.12 cPs), and the surface tension lower (22.5 dyne/cm). Both these factors favor the formation of smooth fibers. Nanofibers spun from DMF had a beaded morphology which is in confirmation of the reported literature.[39] The formation of beads can be attributed to the high surface tension (36.3 dyne/cm) and low viscosity (15.86 cPs) of DMF (vs. ethanol). PVP nanofibers spun from the binary mixture of ethanol/DMF had small diameters (100–350 nm), with average diameter of 200 nm [Fig. 3(C)]. This reduction in fiber size can be attributed to the presence of DMF, which shows an electrolyte behavior that dissociates positive and negative charges.[39,40] DMF facilitates dissolution of charged PVP by separating the ion pairs and increasing the charge density, promoting the formation of thin nanofibers. The values of the fiber diameters with respect to the processing parameters studied (flow rate, voltage, solvent type, concentration, and the presence/absence of salt) is given in Table I.

Synthesis of PVP/PPy composite nanofibers

The optimized parameters required to fabricate thin and smooth nanofibers of PVP/PPy composite were derived from the PVP studies (polymer concentration, solvent, potential, and feed rate). The formation of PVP/PPy composite nanofibers was carried out using two different methods. In the single step method, $FeCl_3$ dissolved in PVP/pyrrole was electrospun using the microfluidic manifold [Fig. 4(B,C)]. For this process, the relative concentration of $FeCl_3$ (10% w/v) was critical for the polymerization of pyrrole into PPy within the fibers. At higher concentrations, $FeCl_3$ crystals are observed along with the formed fibers on the target, while, at lower concentrations, the amount of PPy formed is reduced. Pyrrole concentration was optimized ($\sim 1M$) to get significant increase in conductivity of composite nanofibers as well as stable electrospinning (Fig. 5). Pyrrole monomer concentration ($\sim 1M$) generated composite nanofibers with conductivity of $\sim 10^{-4}$ S/cm, which is an increase of 8 orders of magnitude over pure PVP ($\sim 10^{-12}$ S/cm). For concentrations $< 1\ M$, the composite PVP/PPy nanofibers did not show any significant increase in conductivity ($\sim 10^{-10}$ S/cm), which may be due to isolated conducting domains of PPy in the PVP matrix in accordance to the percolation results reported by Bhat et al.[25] As shown by SEM and TEM [Figs. 4(B,C) and 6(A)], PVP/PPy composite nanofibers are uniform and smooth without any beads. The diameters of the nanofibers range from 70 to 200 nm ($d_{ave} \sim 100$ nm). This bead-free morphology can be attributed to the solvent composition of Ethanol/DMF (1 : 1), which has reduced surface tension. Also, the presence of $FeCl_3$ gives rise to increased charge density of the jet, resulting in higher elongation forces on the jet and promoting the formation of thinner uniform fibers. In the one-step technique, pyrrole polymerizes uniformly in the PVP matrix. As observed from the TEM, PPy forms a continuous uniform phase in the PVP matrix [Fig. 6(A)]. Polymerization of pyrrole was also confirmed from FTIR-ATR analysis. The FTIR spectrum reveals characteristic PPy peaks at 1550, 1470, 1410, 1350, 1208, 1097, 1049, 925, 870, 797, and 730/cm^{-1} [41,42] (Fig. 7). The bulk conductivity of the one-step fabricated nanofibrous mat, calculated using the two-probe method, was $\sim 10^{-4}$ S/cm. The conductivity can be attributed to continuous conduction paths formed by the polypyrrole molecules in the PVP host matrix. Stretching during the electrospinning process may also induce increased charge

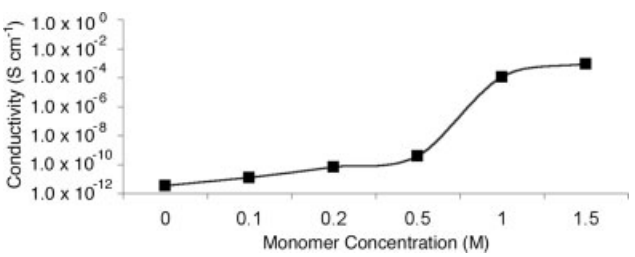

Figure 5 DC conductivity values of composite nanofiber webs as a function of pyrrole monomer concentration.

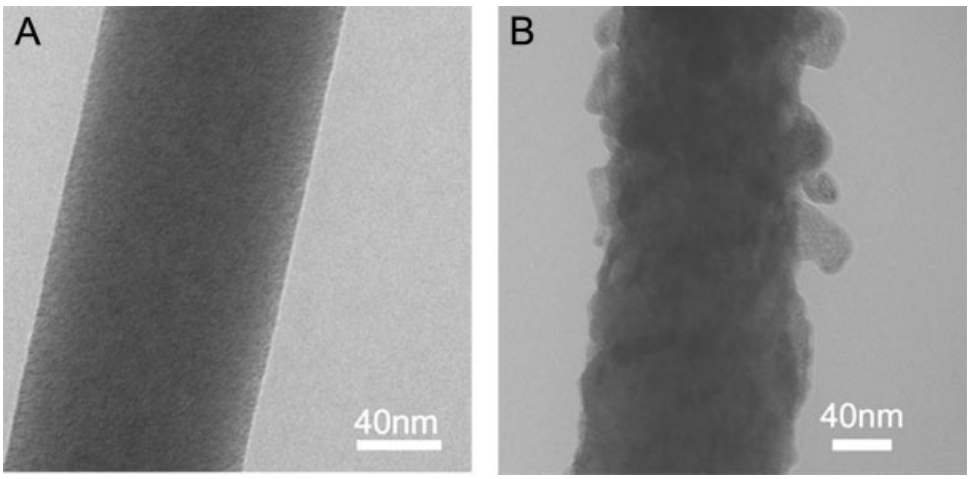

Figure 6 (A) TEM of one-step fabricated PVP/PPy composite nanofiber showing uniform phase of pyrrole in the PVP matrix (B) TEM of vapor phase polymerized PVP/PPy composite nanofiber showing the accumulation of polypyrrole on the surface of PVP nanofiber.

carrier mobility due to orientation of molecules along the fiber-axis.

Figure 4(A) shows an SEM image of PVP/PPy nanofibers formed by two-step electrospinning. PVP nanofibers were initially spun with $FeCl_3$, and subsequently exposed to pyrrole vapors, visually turning black, indicative of the polymerization of pyrrole. The exposure times were varied from 3 h to 10 days. During the first few hours of polymerization (<24 h), the monomer diffusion is fast as revealed by increase in surface conductivity from $\sim 10^{-12}$ to 10^{-3} S/cm (four-probe conductivity). Nanofibers of PVP exposed to pyrrole vapors for more than 24 h did not show any further increase in surface conductivity, indicating that at a later stage of polymerization (>24 h), the surface of PVP nanofibers is saturated with PPy, and further exposure leads to clusters of PPy on the surface as seen from the TEM [Fig. 6(B)]. The surface polymerization of pyrrole inhibits the diffusion of pyrrole monomer into the bulk of the PVP polymer. In contrast to the one-step method, PVP/PPy nanofibers produced using this two-step technique did not show any significant increase in bulk conductivity ($\sim 10^{-8}$ S/cm), which supports our observation from TEM [Fig. 6(B)] indicating polymerization of pyrrole mainly on the surface of PVP, not in the bulk of the fiber. The SEM image [Fig. 4(A)] of the vapor phase polymerized PVP/PPy composite nanofibers reveals nonuniform polymerization of pyrrole in the nanofibrous PVP web. The diameters of the two-step synthesized nanofibers range from 100 to 350 nm with a $d_{ave} \sim 250$ nm, which is higher than the one-step synthesized PVP/PPy nanofibers. Of the two methods, the one-step electrospinning is a facile route to fabricate thin uniform nanofibers with higher bulk conductivity.

CONCLUSIONS

In this work, we report on the successful development a microfluidic source for the electrospinning of nanofibers of PVP and its composite with PPy. The PDMS-based microfluidic device enables multijet spinning source, and also has the advantage of rapid prototyping. It was demonstrated that the morphology and dimension of the nanofibers can be modified by adjusting the polymer concentration, surface tension, salt, strength of the potential, and feed rate. From the processing-structure relationship study, a standard set of parameters required to spin thin smooth, bead-free PVP nanofibers was established and applied to spin composite nanofibers of PVP/PPy. Using the single-step electrospinning technique, conducting composite nanofibers of PVP and PPy were successfully synthesized. The PVP/PPy nanofibers were long and smooth with an average diame-

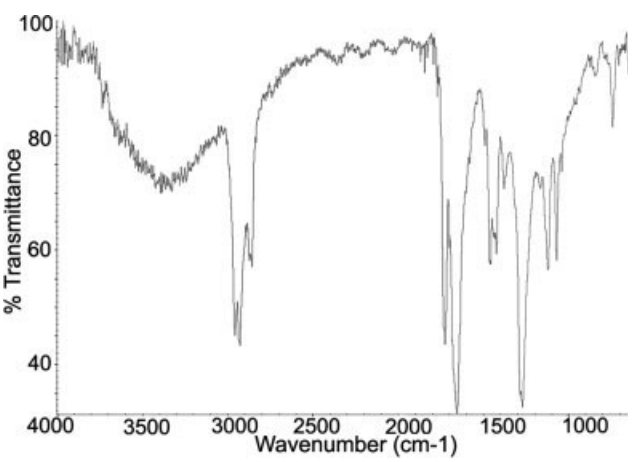

Figure 7 FTIR of PVP/PPy composite nanofibers.

ter of 100 nm. The polymerization of pyrrole in the PVP matrix not only provides a conducting–insulating composite nanostructure, but also improves the processibility of PPy. Conducting, composite nanofibers of physiologically compatible and environmentally stable polymers will likely have potential applications in a diverse range of products, including biosensors, molecular electronics, and smart conductive fabrics.

We would like to acknowledge Ignacio Loscertales (Escuela de Ingenieros Industriales, University of Málaga; Málaga, Spain) and Rodrigo Bocanegra (University of Sevilla; Seville, Spain) for helpful conversations pertaining to the design of the microfluidic electrospinning manifold.

References

1. Formhals, A. U.S. Pat. 1,975, 504 (1934).
2. Reneker, D. H.; Chun, I. Nanotechnology 1996, 7, 216.
3. Sun, Z. C.; Zussman, E.; Yarin, A. L.; Wendorff, J. H.; Greiner, A. Adv Mater 2003, 15, 1929.
4. Li, D.; Xia, Y. N. Nano Lett 2004, 4, 933.
5. Loscertales, I. G.; Barrero, A.; Marquez, M.; Spretz, R.; Velarde-Ortiz, R.; Larsen, G. J Am Chem Soc 2004, 126, 5376.
6. Kameoka, J.; Craighead, H. G. Appl Phys Lett 2003, 83, 371.
7. Bognitzki, M.; Hou, H. Q.; Ishaque, M.; Frese, T.; Hellwig, M.; Schwarte, C.; Schaper, A.; Wendorff, J. H.; Greiner, A. Adv Mater 2000, 12, 637.
8. Yarin, A. L.; Zussman, E. Polymer 2004, 45, 2977.
9. Li, D.; Wang, Y. L.; Xia, Y. N. Nano Lett 2003, 3, 1167.
10. Theron, A.; Zussman, E.; Yarin, A. L. Nanotechnology 2001, 12, 384.
11. He, C. H.; Gong, J. Polym Degrad Stab 2003, 81, 117.
12. Ko, F.; Gogotsi, Y.; Ali, A.; Naguib, N.; Ye, H. H.; Yang, G. L.; Li, C.; Willis, P. Adv Mater 2003, 15, 1161.
13. Dror, Y.; Salalha, W.; Khalfin, R. L.; Cohen, Y.; Yarin, A. L.; Zussman, E. Langmuir 2003, 19, 7012.
14. Dosunmu, O. O.; Chase, G. G.; Kataphinan, W.; Reneker, D. H. Nanotechnology 2006, 17, 1123.
15. Theron, S. A.; Yarin, A. L.; Zussman, E.; Kroll, E. Polymer 2005, 46, 2889.
16. Tomaszewski, W.; Szadkowski, M. Fibres and Textiles in Eastern Europe 2005, 13, 22.
17. Ding, B.; Kimura, E.; Sato, T.; Fujita, S.; Shiratori, S. Polymer 2004, 45, 1895.
18. Potje-Kamloth, K. Crit Rev Anal Chem 2002, 32, 121.
19. Brahim, S.; Narinesingh, D.; Guiseppi-Elie, A. Biosens Bioelectron 2002, 17, 53.
20. Jang, S. Y.; Seshadri, V.; Khil, M. S.; Kumar, A.; Marquez, M.; Mather, P. T.; Sotzing, G. A. Adv Mater 2005, 17, 2177.
21. Bognitzki, M.; Frese, T.; Steinhart, M.; Greiner, A.; Wendorff, J. H.; Schaper, A.; Hellwig, M. Polym Eng Sci 2001, 41, 982.
22. Li, D.; Xia, Y. N. Nano Lett 2003, 3, 555.
23. Diaz, A. F.; Hall, B. IBM J Res Dev 1983, 27, 342.
24. Diaz, F.; Kanazawa, K. K. In Polypyrrole: An Electrochemical Approach to Conducting Polymers, Extended Linear Chain Compounds; Miller, J. S., Ed.; Plenum Press: New York, 1982; Vol. 3, p 417.
25. Bhat, N. V.; Shaikh, Y. B. J Appl Polym Sci 1994, 53, 187.
26. Norris, I. D.; Shaker, M. M.; Ko, F. K.; MacDiarmid, A. G. Synth Met 2000, 114, 109.
27. Xin, Y.; Huang, Z. H.; Yan, E. Y.; Zhang, W.; Zhao, Q. Appl Phys Lett 2006, 89.
28. Wei, M.; Lee, J.; Kang, B. W.; Mead, J. Macromol Rapid Commun 2005, 26, 1127.
29. Nair, S.; Natarajan, S.; Kim, S. H. Macromol Rapid Commun 2005, 26, 1599.
30. Winther-Jensen, B.; Chen, J.; West, K.; Wallace, G. Macromolecules 2004, 37, 5930.
31. McDonald, J. C.; Duffy, D. C.; Anderson, J. R.; Chiu, D. T.; Wu, H. K.; Schueller, O. J. A.; Whitesides, G. M. Electrophoresis 2000, 21, 27.
32. Chronakis, I. S.; Grapenson, S.; Jakob, A. Polymer 2006, 47, 1597.
33. Jun, Z.; Hou, H. Q.; Schaper, A.; Wendorff, J. H.; Greiner, A. e-Polymers 2003, 9, 1.
34. Fong, H.; Chun, I.; Reneker, D. H. Polymer 1999, 40, 4585.
35. Deitzel, J. M.; Kleinmeyer, J.; Harris, D.; Tan, N. C. B. Polymer 2001, 42, 261.
36. Zong, X. H.; Kim, K.; Fang, D. F.; Ran, S. F.; Hsiao, B. S.; Chu, B. Polymer 2002, 43, 4403.
37. Taylor, G. I. Proc R Soc London Ser A 1964, 280, 383.
38. Taylor, G. I. Proc R Soc London Ser A 1969, 313, 453.
39. Yang, Q. B.; Li, Z. Y.; Hong, Y. L.; Zhao, Y. Y.; Qiu, S. L.; Wang, C.; Wei, Y. J Polym Sci Part B: Polym Phys 2004, 42, 3721.
40. Mark, H. F.; Bikales, N. M.; Overburger, C.G.; Menges, G. Encyclopedia of Polymer Science and Engineering, 2nd ed.; Wiley-Interscience: New York, 1985.
41. Kostic, R.; Rakovic, D.; Stepanyan, S. A.; Davidova, I. E.; Gribov, L. A. J Chem Phys 1995, 102, 3104.
42. Omastova, M.; Pavlinec, J.; Pionteck, J.; Simon, F.; Kosina, S. Polymer 1998, 39, 6559.